The RNA polymerase II subunit Rpb9 activates *ATG1* transcription and autophagy

Ting Huang[1], Gaoyue Jiang[1], Yabin Zhang[1], Yuqing Lei[1], Shiyan Liu[1], Huihui Li[2] & Kefeng Lu[1,*] (iD)

Abstract

Macroautophagy/autophagy is a conserved process in eukaryotic cells that mediates the degradation and recycling of intracellular substrates. Proteins encoded by autophagy-related (*ATG*) genes are essentially involved in the autophagy process and must be tightly regulated in response to various circumstances, such as nutrient-rich and starvation conditions. However, crucial transcriptional activators of ATG genes have remained obscure. Here, we identify the RNA polymerase II subunit Rpb9 as an essential regulator of autophagy by a high-throughput screen of a *Saccharomyces cerevisiae* gene knockout library. Rpb9 plays a crucial and specific role in upregulating *ATG1* transcription, and its deficiency decreases autophagic activities. Rpb9 promotes *ATG1* transcription by binding to its promoter region, which is mediated by Gcn4. Furthermore, the function of Rpb9 in autophagy and its regulation of *ATG1/ULK1* transcription are conserved in mammalian cells. Together, our results indicate that Rpb9 specifically activates *ATG1* transcription and thus positively regulates the autophagy process.

Introduction

Macroautophagy (hereafter referred to as autophagy) is a highly conserved process through which superfluous cytoplasmic components or damaged organelles are delivered to vacuoles (in yeast and plants) or lysosomes (in mammals) for degradation and recycling (Wang & Klionsky, 2003; Onodera & Ohsumi, 2005). Evolutionally conserved autophagy-related (*ATG*) proteins are involved in the entire process of autophagy, including initiation, vesicle nucleation, elongation, completion, fusion, and degradation (Takeshige *et al*, 1992; Tsukada & Ohsumi, 1993; Parzych *et al*, 2018). The autophagy process starts with the formation of a phagophore (Yu *et al*, 2018), an initial double-layered membrane structure called the pre-autophagosomal structure (PAS) that sequentially grows into a sealed autophagosome (Suzuki *et al*, 2001). The completed autophagosome finally fuses with vacuoles/lysosomes and is degraded together with sequestered cargos (Xie & Klionsky, 2007). Autophagy is essential for cell homeostasis and cell survival under hostile conditions, such as starvation (Shi *et al*, 2012; Nixon, 2013). Dysregulation, especially downregulation of autophagy, is related to various human pathologies, such as neurodegenerative diseases, cancer, microbial infection, and metabolic diseases (Huang & Klionsky, 2007; Fullgrabe *et al*, 2014; Feng *et al*, 2015; Xie *et al*, 2015).

In mammalian cells, autophagy occurs at low basal levels under normal conditions, and under stress conditions, such as nutrient deficiency, hypoxia, pathogen infection, and autophagy are rapidly and dramatically upregulated (Jin *et al*, 2014; Levine & Kroemer, 2019; Kawabata & Yoshimori, 2020). In yeast, bulk autophagy is inhibited under nutrient-rich conditions. A special type of selective autophagy, the cytoplasm-to-vacuole targeting (Cvt) pathway, occurs in yeast cells when external nutrients are available. The Cvt pathway selectively targets and transfers cytoplasmic hydrolase proteins, including Ape1, Ams1, and Ape4, to vacuole (Klionsky *et al*, 1992; Harding *et al*, 1995; Hutchins & Klionsky, 2001; Yuga *et al*, 2011). The Cvt pathway is biosynthetic rather than degradative, as the hydrolases are transported into vacuoles for biological functions instead of being degraded (Baba *et al*, 1997). Cvt cargos are recruited into a special type of autophagosome, which is usually smaller (approximately 150 nm) than starvation-induced autophagosomes (approximately 500 nm) (Mizushima & Klionsky, 2007; Sawa-Makarska *et al*, 2014). The Cvt pathway requires the common core autophagic machinery and specific receptors Atg19 and Atg11 (Yorimitsu & Klionsky, 2005; Sawa-Makarska *et al*, 2014). As a dynamic process, autophagy is tightly regulated by gene transcription and translation (Delorme-Axford & Klionsky, 2018). At the transcriptional level, many studies have discovered the mechanisms of transcriptional repression on autophagy genes, and how this repression is released by upstream kinases (Jin *et al*, 2014; Bernard *et al*, 2015a, 2015b). In particular, Atg8, a lipid-conjugated ubiquitin-like protein that constitutes an expanding structure of autophagy (Xie *et al*, 2008), is negatively regulated by the transcriptional repressor Ume6, a subunit of the Rpd3 histone deacetylase complex (Bartholomew *et al*, 2012). Atg9, the only transmembrane

1 Department of Neurosurgery, State Key Laboratory of Biotherapy, West China Hospital, Sichuan University, Chengdu, China
2 West China Second University Hospital, Sichuan University, Chengdu, China
*Corresponding author. Tel: +86 13146162934; E-mail: lukf@scu.edu.cn

protein that functions in autophagosome formation by cycling lipid resources (Reggiori *et al*, 2005), is inhibited by the transcriptional repressor Pho23-Rpd3 histone deacetylase complex (Jin & Klionsky, 2014). Histone demethylase Rph1 is a negative transcriptional regulator of several *ATG* genes (mostly obvious on *ATG7*), and this process is dependent on its DNA binding activity but not histone demethylase activity (Bernard *et al*, 2015a, 2015b). Under autophagy-induction conditions, such as nitrogen starvation, the protein kinase Rim15 inhibits Ume6 and Rph1 by phosphorylation, thus releasing the transcriptional repression of *ATG* genes, such as *ATG7*, *ATG8*, and *ATG9* (Bartholomew *et al*, 2012; Bernard *et al*, 2015a, 2015b; Kim *et al*, 2021). Compared to the discovery of transcriptional repressors, the transcriptional activators of *ATG* genes, on the other hand, remain less characterized. The protein serine/threonine kinase Atg1 is essential for the initiation step of PAS (Suzuki *et al*, 2007; Cheong *et al*, 2008; Kawamata *et al*, 2008) and thus functions as the most upstream factor for autophagy induction. However, the transcriptional activation of *ATG1* is largely unknown.

Here, based on a high-throughput screen for novel autophagy factors in *Saccharomyces cerevisiae*, we identified Rpb9, a subunit of RNA polymerase II, that exerted a critical and conserved role in autophagy. Rpb9 deficiency caused the specific blockage of transcriptional induction of *ATG1* and thus led to inhibition of autophagy under starvation conditions. Restoring *ATG1* expression restored autophagy in Rpb9-deficient yeast cells. Mechanistically, Rpb9 is bound to the promoter region of *ATG1* through transcriptional factor Gcn4. A similar function of the Rpb9 ortholog POLR2I on *ULK1* transcription was found in mammalian cells, indicating that the regulation of *ATG1/ULK1* by Rpb9/POLR2I was conserved.

Results

Transcriptional activation is pivotal for the autophagy process

Autophagy is basically a stress-responsive process that is maintained at low levels under normal conditions, such as nutrient-rich conditions and is rapidly induced upon conditions of stress, such as starvation. We first tried to verify whether and how much transcription is involved in autophagy activation. Autophagy can be greatly induced by the Tor1 inhibitor rapamycin (Benjamin *et al*, 2011) or by nitrogen starvation (SD-N) (Tsukada & Ohsumi, 1993; Liu *et al*, 2021). Under rapamycin treatment or SD-N starvation conditions, cycloheximide (CHX) was added to inhibit the synthesis of new proteins in cells, and autophagy activity was determined by GFP processing assays. When GFP-tagged autophagic substrates, such as polyQ (polyglutamine) protein or Atg8, are transferred into vacuoles by autophagy for degradation, the GFP moiety is released and accumulates, as it is highly stable and resists degradation by hydrolases in vacuoles (Klionsky *et al*, 2021a, 2021b). Autophagy was greatly induced by rapamycin or SD-N, as shown by the appearance of GFP moieties, and this effect was completely inhibited by the addition of CHX (Fig 1A), indicating that autophagy induction depends on the synthesis of new proteins. Furthermore, we used thiolutin, a potent inhibitor of RNA polymerases (Pelechano & Perez-Ortin, 2008), to block gene transcription under these conditions. The results showed that thiolutin completely inhibited autophagy induced by rapamycin

or SD-N (Fig 1B), suggesting that transcriptional activation was indeed essential for autophagy. To determine whether the transcriptional activation of *ATGs* occurs rapidly, we treated yeast cells with thiolutin followed by autophagy induction by rapamycin or SD-N. The results showed that short-term induction (3 h) was sufficient to activate autophagy, demonstrating that the transcriptional induction of *ATGs* occurred quite rapidly (Figs 1C–E). Genome mRNA expression sequencing of yeast cells before and after starvation was performed (Fig 1F). The results showed that *ATG1* was the most upregulated among the autophagy genes (Fig 1G and Dataset EV1). In addition, we confirmed the transcription of *ATG* genes by quantitative real-time polymerase chain reaction (qRT-PCR) and the protein levels of Atg proteins, demonstrating upregulation of *ATG1* (Figs 1H and EV1A). After blocking the autophagic degradation of Atg1 (Alemu *et al*, 2012; Kraft *et al*, 2012; Nakatogawa *et al*, 2012; Lin *et al*, 2018), the protein levels of Atg1 were shown to be obviously induced upon starvation (Fig EV1B). Using galactose-controlled promoter, results showed that induced transcription of ATG1 was important for autophagy activities (Fig EV1C–E).

Together, these results suggested that autophagy induction requires prompt transcriptional activation, and *ATG1* gene upregulation is the most obvious effect.

Rpb9 is essential for autophagosome formation

To explore new transcription factor functions in autophagy, we performed a genome-wide screen with the yeast gene knockout collection (Zhang *et al*, 2021) (Fig 2A and Dataset EV2). Using this screen, we identified Rpb9, a subunit of RNA polymerase II (Kaster *et al*, 2016), as a novel candidate for essential autophagy factors (Dataset EV2). Next, we confirmed that Rpb9 deficiency blocked autophagy to a similar extent as Atg1 deficiency and that re-expression of Rpb9 restored autophagy by detecting the autophagic degradation of different substrates GFP-50Q (Shen *et al*, 2021; Zhang *et al*, 2021), GFP-Atg8 (Araki *et al*, 2017; Klionsky *et al*, 2021a, 2021b), and GFP-Pgk1 (Welter *et al*, 2010) (Figs 2B and EV2A and B). Starvation resistance is deficient in yeast cells with dysfunctional autophagy (Tsukada & Ohsumi, 1993; Zhang *et al*, 2021). Rpb9 deficiency caused loss of starvation resistance after nitrogen starvation (Fig 2C). Cherry-Atg8 can be transferred into vacuoles by autophagy induced by starvation in WT yeast cells. However, deletion of essential factors for autophagosome formation, such as Atg1, caused the diffuse cytoplastic distribution of Atg8 and deletion of the SNARE protein Vam3, which is responsible for autophagosome-vacuole fusion (Moreau *et al*, 2013; van der Beek *et al*, 2019), caused dot-like (autophagosome) distribution of Atg8 (Figs 2D and E, and EV2C). Rpb9 deletion caused the diffuse cytoplastic distribution of Atg8 similar to that noted in Atg1 deletion, suggesting that Rpb9 is essential for autophagosome formation instead of fusion (Figs 2D and E, and EV2C). Ape1 (RFP tagged), another classic autophagic substrate, cannot be transported into vacuoles in Rpb9-deleted yeast cells, which is similar to that noted in Atg1-deleted cells (Figs 2F and EV2D). Furthermore, a quantitative alkaline phosphatase assay (Araki *et al*, 2017) showed that Rpb9 deficiency blocked the autophagic transfer of the substrate Pho8Δ60 to a similar extent as deletion of the essential autophagy factor Atg8 (Figs 2G and EV2E). Vacuole maturation of Ape1 by autophagy under rich-medium conditions was also found to be

blocked in Rpb9-deleted yeast cells (Fig EV2F). After determining that Rpb9 regulates autophagosome formation instead of fusion steps (Fig 2D and E), we then tried to analyze which processes of autophagosome formation are regulated by Rpb9. Results showed that Atg1/Atg13 puncta but not Atg9 recruitment or membrane

elongation (Atg12-Atg5 conjugation system) was regulated by Rpb9 (Fig EV2G–J).

The endocytosis pathway targets and transfers endocytic substrates, such as plasma membrane protein Sna3, to vacuoles for degradation, and the vacuole sorting pathway transfers proteins,
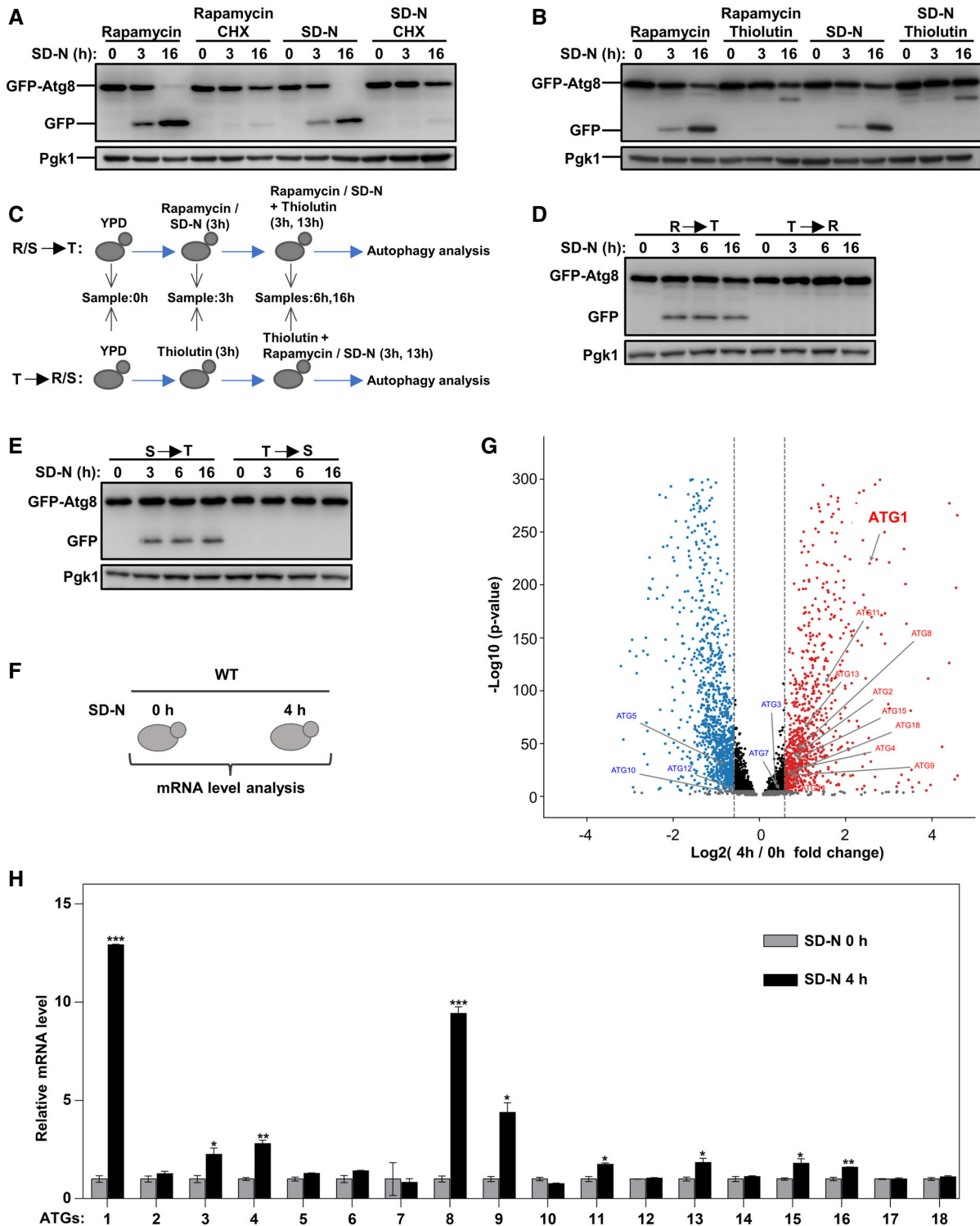

Figure 1.

Figure 1. Autophagy activation is dependent on gene transcription.

A, B   After grown in nutrient-rich medium to log phase, wild-type (WT) cells were treated with rapamycin (10 μM) or subject to nitrogen starvation (SD-N) for 3 and 16 h and degradation of autophagic marker GFP-Atg8 was detected. The cycloheximide (CHX, 100 μg/ml) or thiolutin (10 μg/ml) was simultaneously used to block protein synthesis or gene transcription.

C–E   Yeast cells were treated with thiolutin (10 μg/ml) together with rapamycin or nitrogen starvation in different order for 3, 6, and 16 h and degradation of autophagic marker GFP-Atg8 was detected.

F   WT cells were grown in YPD to log phase and then cultured in SD-N media for 4 h. Collected yeast cells were subject to genome mRNA sequencing and quantification.

G   Genome-wide analysis of differential gene expression in yeast cells cultured in SD-N compared to cells in rich medium (P-value < 0.05, blue: downregulated, red: upregulated). Significance was determined by one-way ANOVA (unpaired) followed by Tukey's multiple comparison test (n = 3 biological replicates).

H   Yeast cells were grown in YPD to log phase and then shifted to SD-N for 4 h. The total RNA was extracted to detect mRNA levels of autophagy genes by qRT-PCR (quantitative real-time polymerase chain reaction). Bars represent mean, error bars represent standard deviation, significance was determined by one-way ANOVA (unpaired) followed by Tukey's multiple comparison test, *indicates $P < 0.05$, **indicates $P < 0.01$, ***indicates $P < 0.001$ (n = 5 biological replicates).

such as carboxypeptidase Y (Cpy1), to vacuoles for hydrolysis function (Yanguas *et al*, 2019). These two vacuole-based pathways were not affected by Rpb9 deletion (Figs 2H and I, and EV2K), indicating that Rpb9 functions specifically in autophagy.

Collectively, we identified and confirmed that Rpb9 is essential for the autophagy process and functions at the autophagosome formation step.

Rpb9 is a specific transcriptional activator of the *ATG1* gene

Although recognized as a subunit of RNA polymerase II, Rpb9 is not an essential factor of RNA polymerase II. Yeast cells with Rpb9 deletion are viable, whereas cells with deletion of other subunits are inviable (Giaever *et al*, 2002). These results require Rpb9 is not required for the general catalytic activity of RNA polymerase II core enzyme. This notion is supported by the observation that deletion of Rpb9 has no effect on the assembly of the RNA polymerase II complex by other subunits (Hull *et al*, 1995). Instead, Rpb9 is involved in the selection of the transcription initiation site (Hull *et al*, 1995; Ziegler *et al*, 2003), control of fidelity (Walmacq *et al*, 2009), transcription-coupled nucleotide-excision repair, and termination of piRNA transcription (Berkyurek *et al*, 2021). We hypothesized that Rpb9 may function in autophagy through specific transcriptional regulation of *ATG* genes. A transcriptomics analysis of WT and Rpb9-deleted yeast cells subjected to nitrogen starvation was performed (Fig 3A). Clustering of differential genes from the transcriptome data showed that deletion of Rpb9 did not cause substantial transcriptional blockage given that the numbers of upregulated and downregulated genes in Rpb9-deficient cells were generally equal (Fig 3B and C). We then focused on the *ATG* genes and found that Rpb9 deletion specifically caused downregulation of *ATG1* (Figs 3C and EV3A and Dataset EV3). The qRT-PCR analysis confirmed that Rpb9 deletion blocked the transcriptional induction of *ATG1* (Figs 3D and EV3B). Consistently, the proteins expression levels of Atg1 were also found to be regulated by Rpb9 (Fig EV3C and D). To further verify that Rbp9 deletion blocked autophagy through the downregulation of *ATG1*, we exogenously overexpressed several *ATG* genes, including *ATG1*, in Rbp9-deleted yeast cells and assessed the restoration of autophagy. The results showed that *ATG1* overexpression restored autophagy in Rbp9-deleted cells, whereas other *ATGs*, such as *ATG5*, *ATG9*, *ATG13*, and *ATG17*, could not (Fig 3E–I). These results suggest that Rpb9 functions in autophagy through specific upregulation of *ATG1* transcription.

Rpb9 functions in autophagy, and the regulation of *ATG1* transcription depends on its N-terminal zinc finger domain and linker region

The protein structure of Rpb9 mainly contains two zinc finger domains with zinc finger 1 (Zn1) and a linker region at the N-terminus and zinc finger 2 (Zn2) at the C-terminus (Figs 4A and EV4A). We then tested the functions of different truncated Rpb9 proteins in autophagy and *ATG1* transcription. The results showed that Zn1 and the linker region together (Rpb9 1–52) were sufficient to restore autophagy in Rpb9-deficient cells, whereas Zn2 deletion had no effect on Rpb9 function in autophagy, as shown by degradation of the autophagic substrate GFP-50Q and starvation resistance (Fig 4A–C). Similarly, overexpression of Zn1 and the linker region together (Rpb9 1–52) restored starvation-induced *ATG1* transcription (Fig 4A and D).

Next, we verified the importance of the Zn1 domain for Rpb9 function in autophagy and *ATG1* transcription using two mutants, one with Zn1 mutations (C10/29/32A, N mutation) and another with Zn2 mutations (C75/78/103/106A, C mutation) (Fig 4A). The results further confirmed that Zn1 was essential for Rpb9 function in autophagy and *ATG1* transcription, whereas Zn2 was not (Fig 4B–D).

Rpb9 regulates *ATG1* transcription through Gcn4

The above results identified Rpb9 as a transcriptional activator of *ATG1*. We then analyzed which regions in the *ATG1* promoter were bound by Rpb9. Chromatin immunoprecipitation (ChIP) assays were performed followed by detecting the Rpb9-binding sites in the upstream (−) and downstream (+) regions of *ATG1* encoding the start site with primers each spanning approximately 100 nucleotides (Fig 5A). The results showed that the −900 base pair (bp), −800 bp, and −700 bp regions upstream of the *ATG1* ORF were enriched in the DNA fragments precipitated by Rpb9 (Fig 5A). This finding indicated that Rpb9 may regulate *ATG1* transcription by binding the −900 to −700 bp upstream of the *ATG1* ORF. However, an electrophoretic mobility shift assay (EMSA) revealed no direct interaction between Rpb9 and these regions (Fig EV4B). We thus hypothesized that Rpb9 may bind the promoter of *ATG1* through interaction with other transcription factors. It has been suggested that the transcription factor Gcn4 regulates Atg1 transcription by binding to its promoter regions (Bernard *et al*, 2015a, 2015b), which were also found to be bound by Rpb9 in our study (Fig 5A). Indeed,

while Rpb9 alone could not bind the *ATG1* promoter (Fig EV4B), it efficiently binds the *ATG1* promoter regions in the presence of Gcn4 (Fig 5B). Consistently, deletion of Gcn4 blocked Atg1 transcription, which is similar to that noted for Rpb9 deletion (Fig 5C). Furthermore, we found that Rpb9 binding to the promoter regions of *ATG1* was dependent on Gcn4 (Fig 5D). These results suggested that Rpb9

regulated *ATG1* transcription through Gcn4. This finding was strengthened by the observation that Rpb9 directly interacted with Gcn4 (Fig 5E). Interestingly, Gcn4 overexpression in Rpb9-deleted cells did not restore autophagy, and similar results were obtained with the reverse scenario (Fig 5F and G). Notably, overexpression of Gcn4 partly restores the autophagic degradation of GFP-50Q in
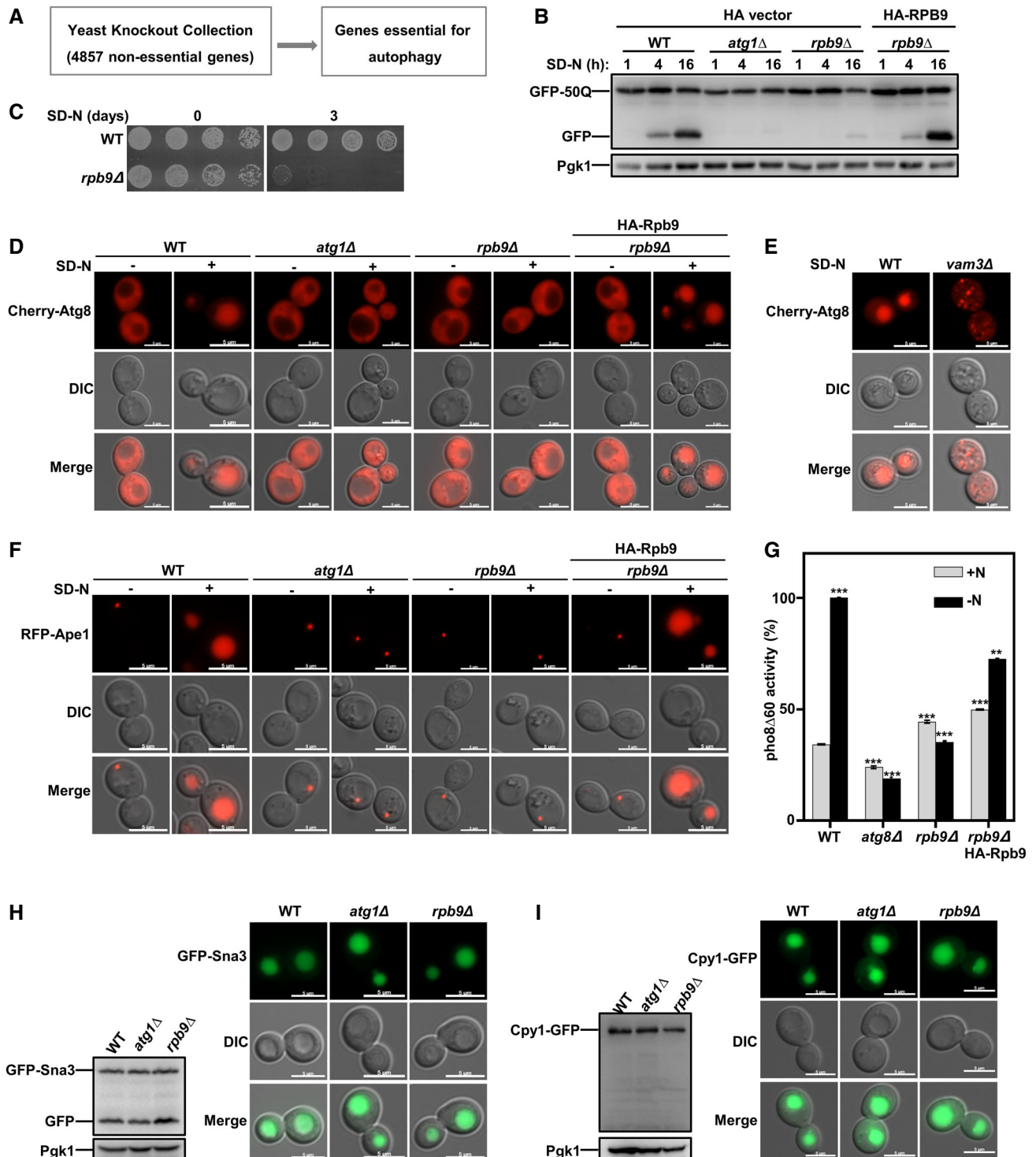
Figure 2.

Figure 2. Rpb9 is essential for the autophagy process.

A   Flow chart of the genome-wide screening of novel essential factors of autophagy in yeast cells. For the screen performance, the knockout library (4,857 non-essential genes) strains were grown on YPD plates followed by starvation on nitrogen-lacking plates for 7 days. After starvation, the yeast cells were re-grown on YPD plates to detect their viability. The potential candidates from this screen were selected based on the starvation-resistance observation (deletion of an autophagy gene causes cell death after starvation).

B   N-terminally GFP-tagged 50Q was checked for its autophagic degradation in indicated yeast cells by GFP processing assays after 1, 4, and 16 h starvation. Yeast cells with *ATG1* deletion were used as positive controls.

C   WT and Rpb9-deleted yeast cells were starved for 3 days in SD-N medium and then detected for cell viability by serial dilution spotting and growth on YPD plates.

D, E   Deficiency of Rpb9 caused blockage of autophagosome formation in yeast cells. Autophagosome marker Cherry-Atg8 expressed in indicated cells was observed by fluorescence microscope before and after nitrogen starvation. In WT yeast cells, Cherry-Atg8 was transferred to vacuoles by autophagy leading to the detection of Cherry signal in vacuoles. The Cherry-Atg8 dots in *vam3Δ* cells showed blockage of autophagosome fusion and diffused cytosolic Cherry-Atg8 in *rpb9Δ* or in *atg1Δ* cells showed blockage of autophagosome formation. Experiments were conducted for at least three times and representative images were shown. Scale bars: 5 μm.

F   Autophagic transport of substrate Ape1 was blocked in Rpb9-deficient cells. Autophagy substrate Ape1 was labeled with RFP and expressed in WT and *rpb9Δ* cells. RFP-Ape1 translocation to vacuoles by the autophagy process leading to the detection of RFP signal in vacuoles and blockage of autophagy in *rpb9Δ* cells caused cytosolic retention of Ape1. Experiments were conducted for at least three times and representative images were shown. Scale bars: 5 μm.

G   Detection of Rpb9-dependent transport of autophagic substrate Pho8Δ60 by ALP assays. Yeast cells were starved for 4 h. Activated Pho8Δ60 activity in vacuoles was measured with indicated cells. Bars represent mean, error bars represent standard deviation, significance was determined by one-way ANOVA (unpaired) followed by Tukey's multiple comparison test, **indicates $P < 0.01$, ***indicates $P < 0.001$ ($n = 5$ biological replicates).

H   Vacuole localization and degradation of endocytosis substrate GFP-Sna3 in WT, *atg1Δ*, and *rpb9Δ* cells. Scale bars: 5 μm.

I   Carboxypeptidases Y (Cpy1), a vacuolar-resident hydrolase, was analyzed for its transporting to vacuoles by the secretory pathway in WT, *atg1Δ*, and *rpb9Δ* cells. Scale bars: 5 μm.

rpb9Δ cells (Fig 5F), while over-expression of Rpb9 in *gcn4Δ* cells failed to have the same effect (Fig 5G). Together with results showing that Rpb9 only binds the ATG1 promoter in the presence of Gcn4 (Figs 5B and EV4B), we speculated that Gcn4 binds the ATG1 promoter and interacts with Rpb9; the latter recruits RNA polymerase II complex through interacting with Rpb1 and Rpb2 subunits. There is a possibility that Gcn4 directly and weakly binds the RNA polymerase II complex in the absence of Rpb9 or that unknown factors other than Rpb9 exist to recruit the RNA polymerase II to ATG1 promoter-bound Gcn4.

These results indicate that both Rpb9 and Gcn4 are necessary for *ATG1* transcription and Rpb9 binds the *ATG1* promoter through Gcn4.

Rpb9 function in autophagy is highly conserved across eukaryotes

Autophagy factors are mostly conserved in eukaryotic cells from yeast to mammalian cells. We tried to analyze whether Rpb9 regulation of autophagy is also conserved. First, we searched for Rpb9 orthologs in other eukaryotes through bioinformatics analysis using a sequence homology algorithm (protein–protein BLAST, BlastP) (Boratyn *et al*, 2012). This search showed highly conserved orthologs of *S. cerevisiae* Rpb9 in other eukaryotic species (Figs 6A and B, and EV5A). All Rpb9 orthologs presented similar domain architectures (Fig 6A). A simple phylogenetic tree indicated the evolutionary conservation of Rpb9 orthologs (Fig 6B). Strikingly, when expressed in yeast cells, Rpb9 orthologs restored the autophagic degradation of the model substrate GFP-50Q (Fig 6C). Similar to yeast Rpb9, the first zinc finger domain plus linker region from Rpb9 orthologs restored autophagy in Rpb9-deleted yeast cells (Fig 6D). Furthermore, Rpb9 orthologs restored the starvation resistance and ATG1 transcription in Rpb9-deleted yeast cells (Fig 6E and F). We next detected the effects of *Homo sapiens* POLR2I on *ATG* genes and found that knockdown of POLR2I in human KEK293T cells specifically reduced the expression of ULK1 (Figs 6G and EV5B), which encodes ULK1, the human ortholog of yeast Atg1. Autophagic activities were reduced by POLR2I knockdown

mammalian cells, which was shown by the reduced degradation of autophagy receptor p62 and less amount of autophagosomes (LC3 puncta) (Fig EV5C and D), indicating the conserved importance of POLR2I for autophagy in mammalian cells.

Together, these results demonstrated that Rpb9 functions in autophagy and that its regulation of *ATG1* transcription is highly conserved in eukaryotic cells.

Discussion

Understanding the prompt and efficient induction of autophagy upon stimulation is one of the major topics of focus in this field. As a quick response to stress conditions, transcription activation is pivotal for the quick and efficient induction of autophagy (Fig 1A–E). Interesting studies on transcriptional regulation of autophagy have revealed transcriptional repressors of autophagy genes. For example, the transcription repressor Ume6 inhibits *ATG8* transcription (Bartholomew *et al*, 2012), the Pho23-Rpd3 histone deacetylase complex inhibits *ATG9* transcription (Jin *et al*, 2014), and the histone demethylase Rph1 inhibits *ATG7* transcription (Bernard *et al*, 2015a, 2015b). However, the transcriptional activators of *ATGs* are less characterized. In this study, we showed that the RNA polymerase II subunit Rpb9 effectively and specifically regulated *ATG1* as a transcriptional activator and thus was essential in the autophagy process.

Given that Rpb9 is an auxiliary subunit of the RNA polymerase II complex (Cramer *et al*, 2000), it is reasonable to assume that Rpb9 may actually regulate *ATG1* transcription by generally regulating transcription in cells. However, several lines of evidence in this study indicated that Rpb9 did not generally affect gene transcription in cells; instead, it exhibited specific regulation of *ATG1*. First, yeast cells with Rpb9 deletion were viable, whereas most of the other subunits of RNA polymerase II were essential for cell growth. Second, the number of upregulated genes in cells harboring a deletion in Rpb9 was similar to the number of downregulated genes (Fig 3A–C). A dramatic downregulation of total gene expression should be observed in Rpb9-deleted cells if Rpb9 was
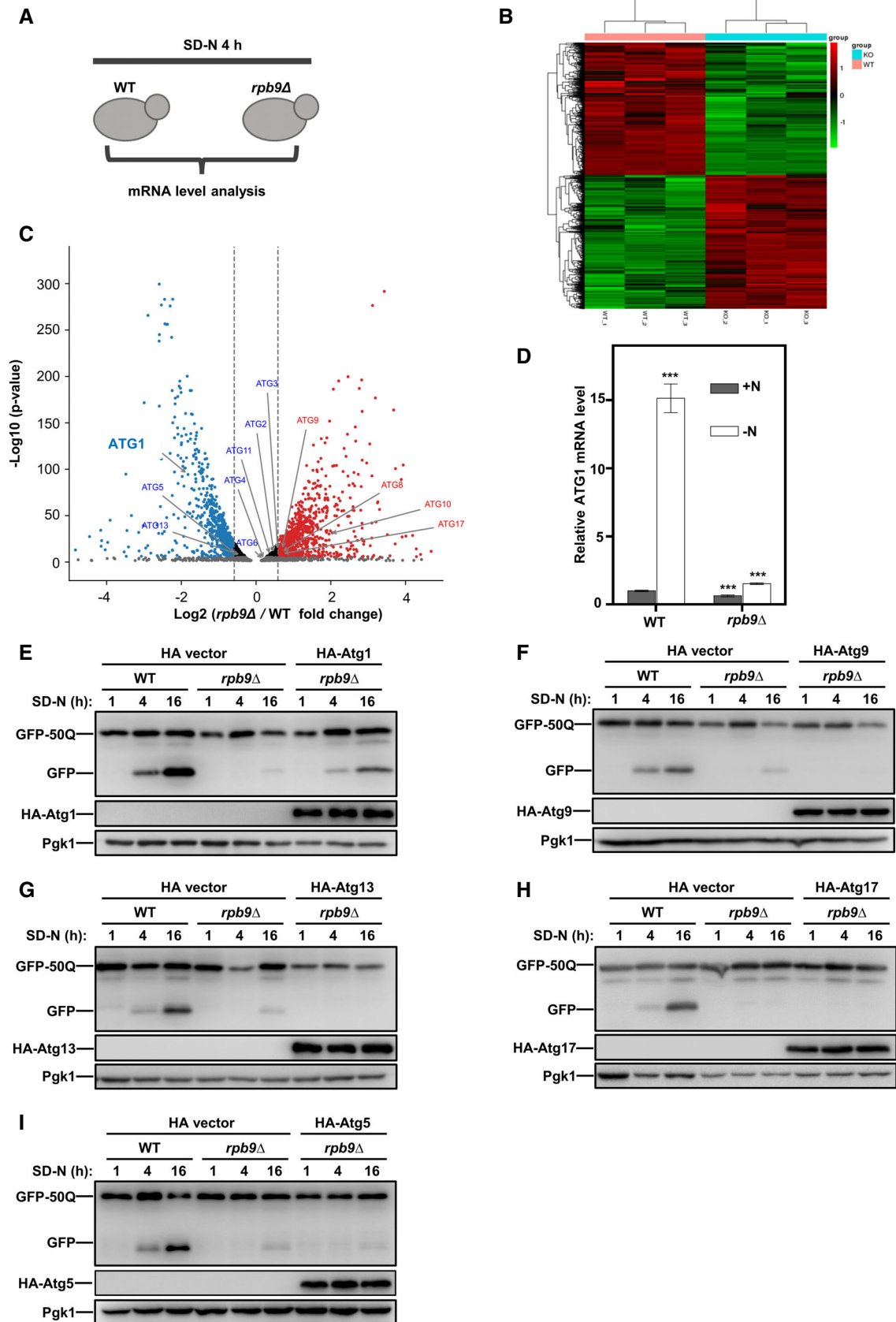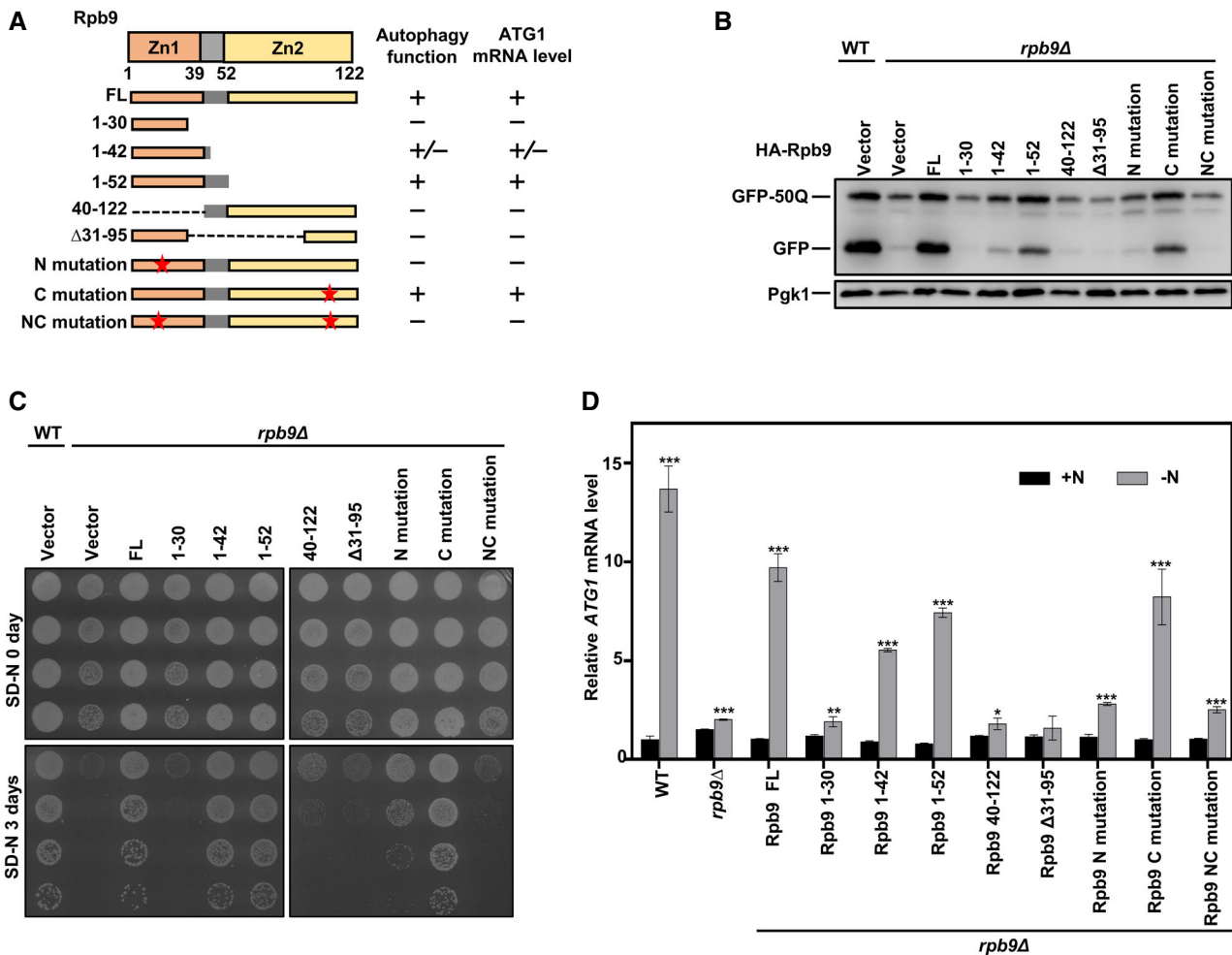
Figure 3.

◄

Figure 3. Rpb9 functions in autophagy through the regulation of *ATG1* transcription.

A WT and Rpb9-deleted yeast cells were grown in YPD to log phase and then cultured in SD-N media for 3 h. Yeast cells were collected and subject to genome mRNA sequencing and quantification.

B Clustered analysis of differential gene sets from RNA-seq data was shown with a heat map.

C Genome-wide analysis of differential gene expression in *rpb9Δ* yeast cells compared to WT cells (*P*-value < 0.05, blue: downregulated, red: upregulated). Significance was determined by one-way ANOVA (unpaired) followed by Tukey's multiple comparison test (*n* = 3 biological replicates).

D WT and *rpb9Δ* yeast cells were grown to log phase in YPD (+N) and then shifted to nitrogen starvation (−N) for 3 h. *ATG1* mRNA levels were quantified by qRT-PCR. Bars represent mean, error bars represent standard deviation, significance was determined by one-way ANOVA (unpaired) followed by Tukey's multiple comparison test, ***indicates *P* < 0.001 (*n* = 5 biological replicates).

E–I Overexpression of *ATG1* could partially restore autophagy in *rpb9Δ* cells. *ATG1*, *ATG9*, *ATG13*, *ATG17*, and *ATG5* were overexpressed in *rpb9Δ* yeast cells, GFP-50Q was checked for its autophagic degradation by GFP processing assays after 1, 4, and 16 h starvation.

Figure 4. The N-terminal zinc figure domain and linker region of Rpb9 are important for its regulation on *ATG1* transcription and autophagy.

A Schematic representation of yeast Rpb9 and indicated truncates checked for function in autophagy and regulation of *ATG1* transcription.

B Indicated Rpb9 truncates and mutants were expressed in *rpb9Δ* cells and autophagic degradation of GFP-50Q was checked by GFP-processing assays.

C The truncates and mutants of the Rpb9 were expressed in *rpb9Δ* yeast cells and cell viability after 3-day starvation in SD-N medium was detected by serial dilution spotting and growth on YPD plates.

D Indicated Rpb9 truncates and mutants were expressed in *rpb9Δ* cells and *ATG1* mRNA levels were analyzed by qRT-PCR. Bars represent mean, error bars represent standard deviation, significance was determined by one-way ANOVA (unpaired) followed by Tukey's multiple comparison test, *indicates *P* < 0.05, **indicates *P* < 0.01, ***indicates *P* < 0.001 (*n* = 5 biological replicates).

involved in general transcription in cells, which was not the case based on what we observed (Fig 3A–C). Third, among the *ATG* genes, Rpb9 deletion caused specific downregulation of *ATG1*

transcription but no other *ATGs* (Fig 3C), further indicating that Rpb9 regulation of *ATG1* was specific. Several *ATGs* were even transcriptionally upregulated in Rpb9-deleted cells (Fig 3C). The
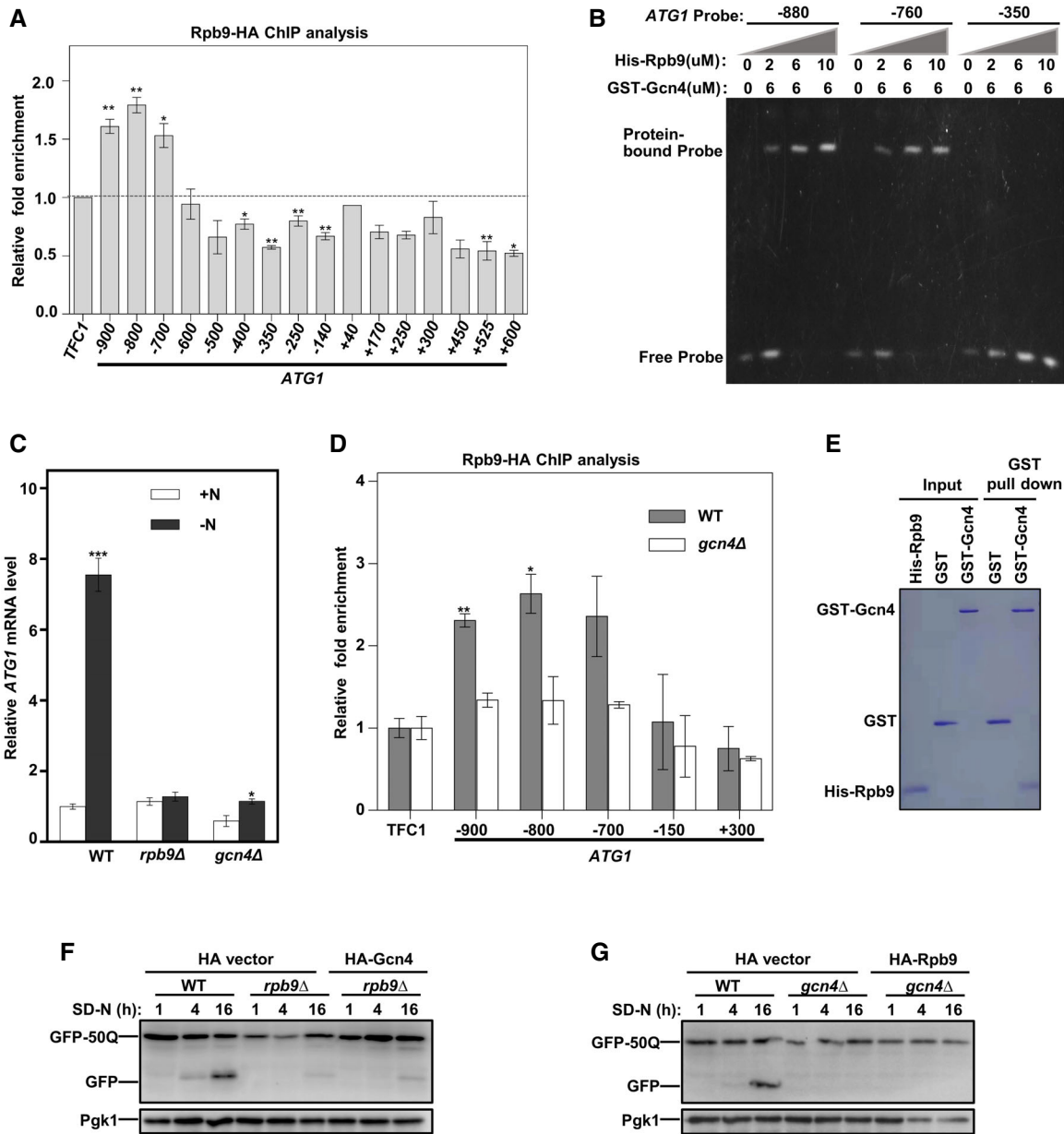
Figure 5. Rpb9 binds the promoter of *ATG1* through Gcn4.

A Chromatin immunoprecipitation (ChIP) assay was performed in Rpb9-HA yeast cells and precipitated DNA was extracted and detected by qRT-PCR analysis with primers spanning the indicated regions upstream and downstream of the *ATG1* starting code. TFC1 was used as negative control. The dotted line indicates no enrichment compared to the control. Bars represent mean, error bars represent standard deviation, significance was determined by one-way ANOVA (unpaired) followed by Tukey's multiple comparison test, *indicates $P < 0.05$, **indicates $P < 0.01$ ($n = 5$ biological replicates).

B His-tagged Rpb9 and GST-tagged Gcn4 were purified from *Escherichia coli* cells and subject to an electrophoretic mobility shift assay (EMSA) together with DNA probes spanning the indicated promoter regions of *ATG1*.

C WT, *rpb9Δ*, and *gcn4Δ* yeast cells were grown to log phase in YPD (+N) and shifted to nitrogen starvation (−N) for 3 h. *ATG1* mRNA levels were quantified by qRT-PCR. Bars represent mean, error bars represent standard deviation, significance was determined by one-way ANOVA (unpaired) followed by Tukey's multiple comparison test, *indicates $P < 0.05$, ***indicates $P < 0.001$ ($n = 5$ biological replicates).

D ChIP assays were performed with WT Rpb9-HA or *gcn4Δ* Rpb9-HA yeast cells followed by qRT-PCR analysis. TFC1 was used as a negative control. Bars represent mean, error bars represent standard deviation, significance was determined by one-way ANOVA (unpaired) followed by Tukey's multiple comparison test, *indicates $P < 0.05$, **indicates $P < 0.01$ ($n = 5$ biological replicates).

E Purified GST-Gcn4 and His-Rpb9 proteins from *E. coli* cells were mixed and GST pulldown assays were performed.

F, G Neither overexpression of Gcn4 in *rpb9Δ* yeast cells nor overexpression of Rpb9 in *gcn4Δ* yeast cells can restore autophagy. Gcn4 or Rpb9 were overexpressed in *rpb9Δ* or *gcn4Δ* yeast cells respectively and autophagic degradation of GFP-50Q was detected.
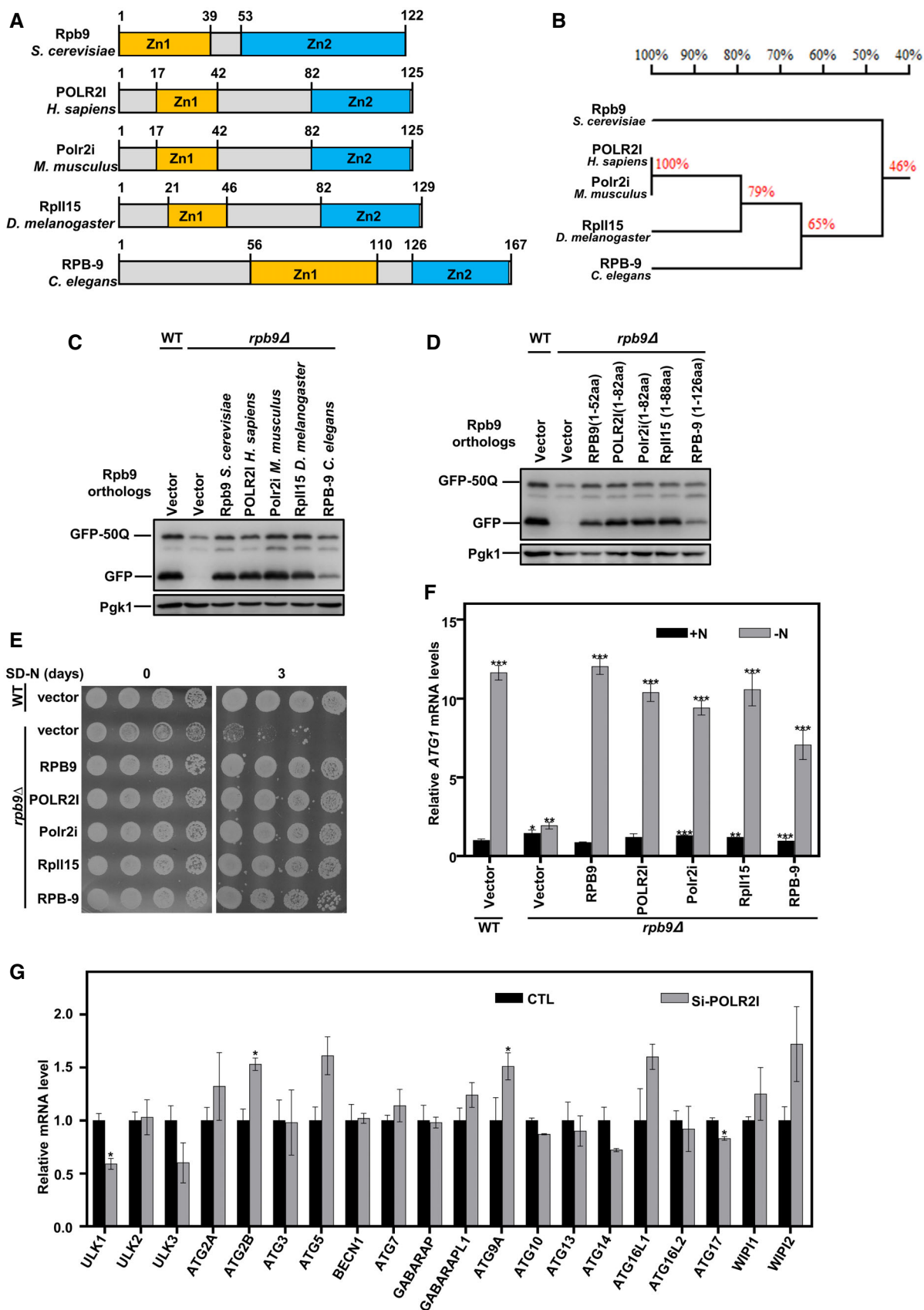
Figure 6.

reason may be that autophagy blockade by Rpb9 deletion would lead to further nutrient limitation under starvation conditions and thus cause further requirements for the autophagy process, as demonstrated by transcriptional activation of *ATGs* other than *ATG1* (Fig 3C). Considering that the mRNA levels of several *ATGs* in addition to *ATG1*, such as *ATG8* and *ATG9*, were dramatically upregulated upon autophagy induction by starvation (Fig 1H), the specific regulation of *ATG1* by Rpb9 further indicated that Rpb9-mediated regulation of *ATG1* was specific.

Prompt induction *ATG* gene transcription is involved in and essential for autophagy induction (Fig 1A–E). Atg1 is located at the convergence of multiple signaling pathways that sense intracellular nutrients, including the TOR (Ma & Blenis, 2009), AMPK, and PKA pathways. Furthermore, Atg1 is essential for initiating autophagosome formation as a very upstream factor in autophagy (Jin *et al*, 2018), and the magnitude of autophagy is partially controlled by the Atg1 levels (Kraft *et al*, 2012; Nakatogawa *et al*, 2012). Thus, the transcriptional upregulation of *ATG1* could cause a robust and prompt induction of autophagy upon starvation. Protein levels of ULK1, the mammalian ortholog of yeast Atg1, are efficiently and specifically downregulated by the E3 ligase NEDD4L through proteasome degradation (Nazio *et al*, 2016; Wang *et al*, 2016); therefore, the transcriptional upregulation of *ULK1/ATG1* is important for the maintenance of autophagy activity during starvation by maintaining sufficient ULK1/Atg1 protein for the autophagy process. This finding is consistent with the observation that Rpb9 function in the transcriptional regulation of *ULK1/ATG1* was conserved, as demonstrated by the observation that expression of Rpb9 orthologs from other eukaryotic species could restore autophagy in Rpb9-deleted yeast cells (Fig 6C). Interestingly, for all the Rpb9 orthologs tested, we found that the first zinc finger domain (Zn1) plus linker region was sufficient to function in autophagy (Fig 6D), and similar results were noted for yeast Rpb9 (Fig 4A). Notably, the Zn1 domain of Rpb9 has been shown to interact with Rpb1 (Cramer *et al*, 2000), a core component of RNA polymerase II. Therefore, we hypothesized that Rpb9 recruits RNA polymerase II to the promoter of *ATG1* by interacting with Rpb1 and DNA-binding protein Gcn4. PLOR2I, the *Homo sapiens* ortholog of Rpb9, is associated with cardiovascular diseases (Talukdar *et al*, 2016), such as hypertensive nephropathy and colorectal cancer (Long *et al*, 2016). Considering the close relationship between autophagy and cardiovascular diseases (Martins *et al*, 2021) and cancers (Klionsky *et al*, 2021a, 2021b), it is possible

that PLOR2I involvement in these diseases is caused by dysregulation of its function in the autophagy process.

In summary, we identified the RNA polymerase II subunit Rpb9 as a pivotal regulator of autophagy that specifically promotes *ATG1* transcriptional activation. Together with previous findings on transcriptional repressors of *ATG* genes, the information provided by this study helps fill the void in our understanding of how *ATG* genes are selectively regulated. In future studies, it will be interesting to uncover the mechanisms by which other *ATGs* are transcriptionally activated after repression is released, especially *ATG8* and *ATG9*, two genes that are also highly induced upon autophagy activation.

Materials and Methods

Yeast strains, media, and constructs

Yeast strains and plasmids used in this study are listed in Tables EV1 and EV2. Standard protocols were used for yeast manipulations. Yeast cells were grown in YPD (1% yeast extract, 2% peptone, and 2% glucose) or synthetic complete (SC) medium (0.67% YNB, 2% glucose, and 0.2% amino acids). For autophagy induction by starvation, yeast cells were cultured to log phase in YPD or SC medium and then switched to nitrogen starvation medium (SD-N; 0.17% yeast nitrogen base without amino acids and ammonium sulfate, supplemented with 2% glucose or galactose or galactose combining with raffinose) for indicated times (h). Chromosomally knockout and tagged strains were constructed by a PCR-based strategy. Standard cloning and site-directed mutagenesis techniques were used.

HEK293T cell culture

Human HEK293T cells were grown in DMEM (supplemented with 10% FBS, 2 mM L-glutamine, and 100 U/ml penicillin-streptomycin) at 37°C with 5% CO_2. Plasmid and siRNA were transfected by Lipofectamine 2000.

Fluorescence microscopy assays

Yeast cells were cultured in SC medium (0.17% YNB, 2% glucose, and 0.2% amino acids) at 30°C. When gowning to log phase, yeast

cells were collected and then washed twice in stilled water, cultured in SD-N media for indicated times at last. Aliquots of liquid culture were collected at indicated time points and allowed to precipitate on concanavalin A coated cover glass for 5 min. Images were captured by Zeiss Observer 7 machine equipped with Apotome. Representative images from at least three independent repeated experiments were shown. HEK293T cells were grown in confocal wells and observed by Zeiss Observer 7 machine equipped with Apotome. Representative images from at least three independent repeated experiments were shown.

Immunoblotting techniques

Collected yeast cells were added to HU lysis buffer (4 M urea, 2.5% SDS, 100 mM Tris-pH 6.8, 0.05 M DTT). They were heated at 65°C to 15 min to prepare protein samples to be resolved on SDS-PAGE gels followed by applying appropriate antibodies and analysis by standard immunoblotting techniques. Monoclonal antibodies against HA-epitope (F-7) and GFP (B-2) were purchased from Santa Cruz Biotechnology (sc-7392 and sc-9996). Monoclonal Pgk1 antibody (22C5; ab113687) was from Abcam. Polyclonal POLR2I antibody (17270-1-AP) was from Proteintech. Monoclonal p62 antibody (EPR4844; ab109012) was from Abcam. Monoclonal GAPDH antibody (60004-1-Ig) was from Proteintech. Polyclonal Ape1 antibody was a gift from Dr. Cong Yi (Zhejiang University).

Genome mRNA expression sequencing

Genome transcriptomics analysis was carried out by Beijing Novogene Bioinformation Technology Co., Ltd. (China). Three independent replicates of wild-type yeast cells before and after starvation or wild-type and Rpb9-deleted yeast cells after starvation were collected. RNAs of yeast cell samples were individually extracted followed by quantification and qualification. A total amount of 3 μg RNA per sample was used as input material. Sequencing libraries were generated using NEBNext® Ultra™ RNA Library Prep Kit for Illumina® (NEB, USA) following the manufacturer's recommendations and index codes were added to attribute sequences to each sample. Briefly, mRNA was purified from total RNA using poly-T oligo-attached magnetic beads. Fragmentation was carried out using divalent cations under elevated temperature in NEBNext First Strand Synthesis Reaction Buffer. First-strand cDNA was synthesized using random hexamer primer and M-MuLV Reverse Transcriptase. Second strand cDNA synthesis was subsequently performed using DNA polymerase I and RNase H. Remaining overhangs were converted into blunt ends via exonuclease/polymerase activities. After adenylation of 3′ ends of DNA fragments, NEB Next Adaptor with hairpin loop structure was ligated to prepare for hybridization. In order to select cDNA fragments of preferentially 150~200 bp in length, the library fragments were purified with the AMPure XP system (Beckman Coulter, Beverly, USA). Then 3 μl USER Enzyme (NEB, USA) was used with size-selected, adaptor-ligated cDNA at 37°C for 15 min followed by 5 min at 95°C before PCR. Then PCR was performed with Phusion High-Fidelity DNA polymerase, Universal PCR primers, and Index (X) Primer. At last, PCR products were purified (AMPure XP system) and library quality was assessed on the Agilent Bioanalyzer 2100 system. The Pearson correlation was analyzed between samples suggesting that the biological

replicates for each experimental group were reliable for further analysis. The data were processed on an online platform (https://magic.novogene.com). Differential expression analysis was performed using the DESeq R package (1.18.0). DESeq provides statistical routines for determining differential expression in digital gene expression data using a model based on the negative binomial distribution. The resulting *P*-values were adjusted using Benjamini and Hochberg's approach for controlling the false discovery rate. Genes with an adjusted *P*-value < 0.05 found by DESeq were assigned as differentially expressed.

RNA extraction and quantitative real-time PCR (qRT-PCR)

Yeast cells were grown in YPD to log phase. Then, Yeast cells were collected and washed twice with distilled water and cultured in SD-N media for the indicated time. Cells were collected and frozen in liquid nitrogen. Cell walls were lysed with the ZYMOLYASE-20T (MP Biomedicals, 320921) and then FastPure cell/tissue total RNA isolation mini kit (Vazyme, RC101-01) was used to extract total RNA. Extracted RNA was converted to cDNA using HiScript III RT SuperMix for qPCR (Vazyme, R323-01) and qRT-PCR reactions were performed using ChamQ Universal SYBR qPCR Master Mix (Vazyme, C711-02) on an iCycler RT-PCR Detection System (Bio-Rad Laboratories). Each assay was performed in triplication for each sample. The reaction mix is in a 15-μl final volume consisting of 7.5 μl of SYBR Green Master mix, 0.5 μl of each primer with 333.3 nM final concentration, 1.5 μl of H_2O, and 5 μl of the cDNA preparation. The thermocycling program is 95°C for 10 min, 40 cycles of 95°C for 15 s, and 60°C for 1 min. After that, melting curves were analyzed to verify PCR specificity. The transcript abundance was analyzed by a comparative threshold-cycle method. The relative abundance of the reference mRNAs of TFC1 was analyzed and taken for normalization of differences in total RNA amount.

Chromatin immunoprecipitation (ChIP)

The strains used in the study were Rpb9-HA, *gcn4Δ* Rpb9-HA. After gowning to the log phase, yeast cells were added with 1% final formaldehyde to perform cross-link of protein-DNA complexes for 20 min at room temperature, and then a working concentration of 0.2 M glycine was added to stop cross-linking. Sample were collected, washed twice in PBS and resuspended in ice-cold FA lysis buffer (50 mM HEPES, pH 7.5, 150 mM NaCl, 1 mM EDTA, 1% Triton X-100, 0.1% sodium deoxycholate, and 0.1% SDS). The cells suspended in lysis buffer were added with zirconia/silica beads (BioSpec, 11079105z) for cell disruption on a multitube bead beater (SCIENTZ) and then were centrifuged 1 min at 1,000 *g* to discard beads. The samples were centrifuged for 15 min at a maximum speed, 4°C. After discarding the supernatant, 1 ml ice-cold FA lysis buffer was added to resuspend the precipitate for sonication (50 cycles of 4 s on, 15 s off, the pulse at 100 W power) at 4°C, and then centrifuged for 15 min at maximum speed 4°C to collect supernatant that was divided into input and IP fractions. One part of the IP fraction was incubated with lgG2a antibody together with protein G-Sepharose beads while the other part was incubated with HA antibody together with protein G-Sepharose beads overnight at 4°C. After immunoprecipitation, the beads were washed serially with FA lysis with 0.5 M NaCl, wash buffer and TE buffer, resuspended in

elution buffer at 65°C metal bath for 10 min. After incubation with RNase A for 1 h at 37°C, the samples were treated with proteinase K for 2 h at 42°C followed overnight at 65°C. The purified DNA was examined by qRT-PCR analysis, which was performed using the ChamQ Universal SYBR qPCR Master Mix.

Statistical analysis

Data are expressed as means ± SD from at least three biological replicates. Statistical analyses were conducted using Prism5. Ordinary one-way or two-way ANOVA with Turkey's multiple comparisons test, or a two-tailed paired or unpaired Student's *t*-test was used to determine statistical significance (*: $P < 0.05$, **: $P < 0.01$, ***: $P < 0.001$, NS: no statistical difference).

Data availability

There is no data deposited in public databases.

Expanded View for this article is available online.

Author contributions

Ting Huang: Conceptualization; methodology. **Gaoyue Jiang:** Methodology. **Yabin Zhang:** Methodology. **Yuqing Lei:** Methodology. **Shiyan Liu:** Methodology. **Huihui Li:** Conceptualization. **Kefeng Lu:** Conceptualization; supervision; funding acquisition; writing – review and editing.

Disclosure and competing interests statement

The authors declare that they have no conflict of interest.

References

Alemu EA, Lamark T, Torgersen KM, Birgisdottir AB, Larsen KB, Jain A, Olsvik H, Overvatn A, Kirkin V, Johansen T (2012) ATG8 family proteins act as scaffolds for assembly of the ULK complex: sequence requirements for LC3-interacting region (LIR) motifs. *J Biol Chem* 47: 39275–39290

Araki Y, Kira S, Noda T (2017) Quantitative assay of macroautophagy using Pho8 big up tri, open60 assay and GFP-cleavage assay in yeast. *Methods Enzymol* 588: 307–321

Baba M, Osumi M, Scott SV, Klionsky DJ, Ohsumi Y (1997) Two distinct pathways for targeting proteins from the cytoplasm to the vacuole/lysosome. *J Cell Biol* 7: 1687–1695

Bartholomew CR, Suzuki T, Du Z, Backues SK, Jin M, Lynch-Day MA, Umekawa M, Kamath A, Zhao M, Xie Z *et al* (2012) Ume6 transcription factor is part of a signaling cascade that regulates autophagy. *Proc Natl Acad Sci USA* 28: 11206–11210

Benjamin D, Colombi M, Moroni C, Hall MN (2011) Rapamycin passes the torch: a new generation of mTOR inhibitors. *Nat Rev Drug Discov* 11: 868–880

Berkyurek AC, Furlan G, Lampersberger L, Beltran T, Weick EM, Nischwitz E, Cunha NI, Braukmann F, Akay A, Price J *et al* (2021) The RNA polymerase II subunit RPB-9 recruits the integrator complex to terminate *Caenorhabditis elegans* piRNA transcription. *EMBO J* 5: e105565

Bernard A, Jin M, Gonzalez-Rodriguez P, Fullgrabe J, Delorme-Axford E, Backues SK, Joseph B, Klionsky DJ (2015a) Rph1/KDM4 mediates nutrient-limitation signaling that leads to the transcriptional induction of autophagy. *Curr Biol* 5: 546–555

Bernard A, Jin M, Xu Z, Klionsky DJ (2015b) A large-scale analysis of autophagy-related gene expression identifies new regulators of autophagy. *Autophagy* 11: 2114–2122

Boratyn GM, Schaffer AA, Agarwala R, Altschul SF, Lipman DJ, Madden TL (2012) Domain enhanced lookup time accelerated BLAST. *Biol Direct* 7: 12

Cheong H, Nair U, Geng J, Klionsky DJ (2008) The Atg1 kinase complex is involved in the regulation of protein recruitment to initiate sequestering vesicle formation for nonspecific autophagy in *Saccharomyces cerevisiae*. *Mol Biol Cell* 2: 668–681

Cramer P, Bushnell DA, Fu J, Gnatt AL, Maier-Davis B, Thompson NE, Burgess RR, Edwards AM, David PR, Kornberg RD (2000) Architecture of RNA polymerase II and implications for the transcription mechanism. *Science* 5466: 640–649

Delorme-Axford E, Klionsky DJ (2018) Transcriptional and post-transcriptional regulation of autophagy in the yeast *Saccharomyces cerevisiae*. *J Biol Chem* 15: 5396–5403

Feng Y, Yao Z, Klionsky DJ (2015) How to control self-digestion: transcriptional, post-transcriptional, and post-translational regulation of autophagy. *Trends Cell Biol* 6: 354–363

Fullgrabe J, Klionsky DJ, Joseph B (2014) The return of the nucleus: transcriptional and epigenetic control of autophagy. *Nat Rev Mol Cell Biol* 1: 65–74

Giaever G, Chu AM, Ni L, Connelly C, Riles L, Veronneau S, Dow S, Lucau-Danila A, Anderson K, Andre B *et al* (2002) Functional profiling of the *Saccharomyces cerevisiae* genome. *Nature* 6896: 387–391

Harding TM, Morano KA, Scott SV, Klionsky DJ (1995) Isolation and characterization of yeast mutants in the cytoplasm to vacuole protein targeting pathway. *J Cell Biol* 3: 591–602

Huang J, Klionsky DJ (2007) Autophagy and human disease. *Cell Cycle* 15: 1837–1849

Hull MW, McKune K, Woychik NA (1995) RNA polymerase II subunit RPB9 is required for accurate start site selection. *Genes Dev* 4: 481–490

Hutchins MU, Klionsky DJ (2001) Vacuolar localization of oligomeric alpha-mannosidase requires the cytoplasm to vacuole targeting and autophagy pathway components in *Saccharomyces cerevisiae*. *J Biol Chem* 23: 20491–20498

Jin M, Klionsky DJ (2014) Transcriptional regulation of ATG9 by the Pho23-Rpd3 complex modulates the frequency of autophagosome formation. *Autophagy* 9: 1681–1682

Jin M, He D, Backues SK, Freeberg MA, Liu X, Kim JK, Klionsky DJ (2014) Transcriptional regulation by Pho23 modulates the frequency of autophagosome formation. *Curr Biol* 12: 1314–1322

Jin S, Zhang X, Miao Y, Liang P, Zhu K, She Y, Wu Y, Liu DA, Huang J, Ren J *et al* (2018) m(6) A RNA modification controls autophagy through upregulating ULK1 protein abundance. *Cell Res* 9: 955–957

Kaster BC, Knippa KC, Kaplan CD, Peterson DO (2016) RNA polymerase II trigger loop mobility: indirect effects of Rpb9. *J Biol Chem* 28: 14883–14895

Kawabata T, Yoshimori T (2020) Autophagosome biogenesis and human health. *Cell Discov* 1: 33

Kawamata T, Kamada Y, Kabeya Y, Sekito T, Ohsumi Y (2008) Organization of the pre-autophagosomal structure responsible for autophagosome formation. *Mol Biol Cell* 5: 2039–2050

Kim B, Lee Y, Choi H, Huh WK (2021) The trehalose-6-phosphate phosphatase Tps2 regulates ATG8 transcription and autophagy in *Saccharomyces cerevisiae*. *Autophagy* 4: 1013–1027

Klionsky DJ, Cueva R, Yaver DS (1992) Aminopeptidase I of *Saccharomyces cerevisiae* is localized to the vacuole independent of the secretory pathway. *J Cell Biol* 2: 287–299

Klionsky DJ, Abdel-Aziz AK, Abdelfatah S, Abdellatif M, Abdoli A, Abel S, Abeliovich H, Abildgaard MH, Abudu YP, Acevedo-Arozena A *et al* (2021a) Guidelines for the use and interpretation of assays for monitoring autophagy (4th edition). *Autophagy* 1: 1–382

Klionsky DJ, Petroni G, Amaravadi RK, Baehrecke EH, Ballabio A, Boya P, Bravo-San PJ, Cadwell K, Cecconi F, Choi A *et al* (2021b) Autophagy in major human diseases. *EMBO J* 19: e108863

Kraft C, Kijanska M, Kalie E, Siergiejuk E, Lee SS, Semplicio G, Stoffel I, Brezovich A, Verma M, Hansmann I *et al* (2012) Binding of the Atg1/ULK1 kinase to the ubiquitin-like protein Atg8 regulates autophagy. *EMBO J* 18: 3691–3703

Levine B, Kroemer G (2019) Biological functions of autophagy genes: a disease perspective. *Cell* 1–2: 11–42

Lin MG, Schoneberg J, Davies CW, Ren X, Hurley JH (2018) The dynamic Atg13-free conformation of the Atg1 EAT domain is required for phagophore expansion. *Mol Biol Cell* 10: 1228–1237

Liu K, Sutter BM, Tu BP (2021) Autophagy sustains glutamate and aspartate synthesis in *Saccharomyces cerevisiae* during nitrogen starvation. *Nat Commun* 1: 57

Long NP, Lee WJ, Huy NT, Lee SJ, Park JH, Kwon SW (2016) Novel biomarker candidates for colorectal cancer metastasis: a meta-analysis of *in vitro* studies. *Cancer Inform* 4: 11–17

Ma XM, Blenis J (2009) Molecular mechanisms of mTOR-mediated translational control. *Nat Rev Mol Cell Biol* 5: 307–318

Martins WK, Silva M, Pandey K, Maejima I, Ramalho E, Olivon VC, Diniz SN, Grasso D (2021) Autophagy-targeted therapy to modulate age-related diseases: success, pitfalls, and new directions. *Curr Res Pharmacol Drug Discov* 2: 100033

Mizushima N, Klionsky DJ (2007) Protein turnover via autophagy: implications for metabolism. *Annu Rev Nutr* 27: 19–40

Moreau K, Renna M, Rubinsztein DC (2013) Connections between SNAREs and autophagy. *Trends Biochem Sci* 2: 57–63

Nakatogawa H, Ohbayashi S, Sakoh-Nakatogawa M, Kakuta S, Suzuki SW, Kirisako H, Kondo-Kakuta C, Noda NN, Yamamoto H, Ohsumi Y (2012) The autophagy-related protein kinase Atg1 interacts with the ubiquitin-like protein Atg8 via the Atg8 family interacting motif to facilitate autophagosome formation. *J Biol Chem* 34: 28503–28507

Nazio F, Carinci M, Valacca C, Bielli P, Strappazzon F, Antonioli M, Ciccosanti F, Rodolfo C, Campello S, Fimia GM *et al* (2016) Fine-tuning of ULK1 mRNA and protein levels is required for autophagy oscillation. *J Cell Biol* 6: 841–856

Nixon RA (2013) The role of autophagy in neurodegenerative disease. *Nat Med* 8: 983–997

Onodera J, Ohsumi Y (2005) Autophagy is required for maintenance of amino acid levels and protein synthesis under nitrogen starvation. *J Biol Chem* 36: 31582–31586

Parzych KR, Ariosa A, Mari M, Klionsky DJ (2018) A newly characterized vacuolar serine carboxypeptidase, Atg42/Ybr139w, is required for normal vacuole function and the terminal steps of autophagy in the yeast *Saccharomyces cerevisiae*. *Mol Biol Cell* 9: 1089–1099

Pelechano V, Perez-Ortin JE (2008) The transcriptional inhibitor thiolutin blocks mRNA degradation in yeast. *Yeast* 2: 85–92

Reggiori F, Shintani T, Nair U, Klionsky DJ (2005) Atg9 cycles between mitochondria and the pre-autophagosomal structure in yeasts. *Autophagy* 2: 101–109

Sawa-Makarska J, Abert C, Romanov J, Zens B, Ibiricu I, Martens S (2014) Cargo binding to Atg19 unmasks additional Atg8 binding sites to mediate membrane-cargo apposition during selective autophagy. *Nat Cell Biol* 5: 425–433

Shen T, Jiang L, Wang X, Xu Q, Han L, Liu S, Huang T, Li H, Dai L, Li H *et al* (2021) Function and molecular mechanism of N-terminal acetylation in autophagy. *Cell Rep* 7: 109937

Shi CS, Shenderov K, Huang NN, Kabat J, Abu-Asab M, Fitzgerald KA, Sher A, Kehrl JH (2012) Activation of autophagy by inflammatory signals limits IL-1beta production by targeting ubiquitinated inflammasomes for destruction. *Nat Immunol* 3: 255–263

Suzuki K, Kirisako T, Kamada Y, Mizushima N, Noda T, Ohsumi Y (2001) The pre-autophagosomal structure organized by concerted functions of APG genes is essential for autophagosome formation. *EMBO J* 21: 5971–5981

Suzuki K, Kubota Y, Sekito T, Ohsumi Y (2007) Hierarchy of Atg proteins in pre-autophagosomal structure organization. *Genes Cells* 2: 209–218

Takeshige K, Baba M, Tsuboi S, Noda T, Ohsumi Y (1992) Autophagy in yeast demonstrated with proteinase-deficient mutants and conditions for its induction. *J Cell Biol* 2: 301–311

Talukdar HA, Foroughi AH, Jain RK, Ermel R, Ruusalepp A, Franzen O, Kidd BA, Readhead B, Giannarelli C, Kovacic JC *et al* (2016) Cross-tissue regulatory gene networks in coronary artery disease. *Cell Syst* 3: 196–208

Tsukada M, Ohsumi Y (1993) Isolation and characterization of autophagy-defective mutants of *Saccharomyces cerevisiae*. *FEBS Lett* 1–2: 169–174

van der Beek J, Jonker C, van der Welle R, Liv N, Klumperman J (2019) CORVET, CHEVI and HOPS - multisubunit tethers of the endo-lysosomal system in health and disease. *J Cell Sci* 132: jcs189134

Walmacq C, Kireeva ML, Irvin J, Nedialkov Y, Lubkowska L, Malagon F, Strathern JN, Kashlev M (2009) Rpb9 subunit controls transcription fidelity by delaying NTP sequestration in RNA polymerase II. *J Biol Chem* 29: 19601–19612

Wang CW, Klionsky DJ (2003) The molecular mechanism of autophagy. *Mol Med* 3–4: 65–76

Wang J, Zhang J, Lee YM, Koh PL, Ng S, Bao F, Lin Q, Shen HM (2016) Quantitative chemical proteomics profiling of de novo protein synthesis during starvation-mediated autophagy. *Autophagy* 10: 1931–1944

Welter E, Thumm M, Krick R (2010) Quantification of nonselective bulk autophagy in *S. cerevisiae* using Pgk1-GFP. *Autophagy* 6: 794–797

Xie Z, Klionsky DJ (2007) Autophagosome formation: core machinery and adaptations. *Nat Cell Biol* 10: 1102–1109

Xie Z, Nair U, Klionsky DJ (2008) Atg8 controls phagophore expansion during autophagosome formation. *Mol Biol Cell* 8: 3290–3298

Xie Y, Kang R, Sun X, Zhong M, Huang J, Klionsky DJ, Tang D (2015) Posttranslational modification of autophagy-related proteins in macroautophagy. *Autophagy* 1: 28–45

Yanguas F, Moscoso-Romero E, Valdivieso MH (2019) Ent3 and GGA adaptors facilitate diverse anterograde and retrograde trafficking events to and from the prevacuolar endosome. *Sci Rep* 1: 10747

Yorimitsu T, Klionsky DJ (2005) Atg11 links cargo to the vesicle-forming machinery in the cytoplasm to vacuole targeting pathway. *Mol Biol Cell* 4: 1593−1605

Yu L, Chen Y, Tooze SA (2018) Autophagy pathway: cellular and molecular mechanisms. *Autophagy* 2: 207−215

Yuga M, Gomi K, Klionsky DJ, Shintani T (2011) Aspartyl aminopeptidase is imported from the cytoplasm to the vacuole by selective autophagy in *Saccharomyces cerevisiae. J Biol Chem* 15: 13704−13713

Zhang H, Zhou J, Xiao P, Lin Y, Gong X, Liu S, Xu Q, Wang M, Ren H, Lu M *et al* (2021) PtdIns4P restriction by hydrolase SAC1 decides specific fusion of autophagosomes with lysosomes. *Autophagy* 8: 1907−1917

Ziegler LM, Khaperskyy DA, Ammerman ML, Ponticelli AS (2003) Yeast RNA polymerase II lacking the Rpb9 subunit is impaired for interaction with transcription factor IIF. *J Biol Chem* 49: 48950−48956